



## Research paper

# Lignin-based activated carbons as metal-free catalysts for the oxidative degradation of 4-nitrophenol in aqueous solution



Maria Martin-Martinez<sup>a</sup>, Maria Filomena F. Barreiro<sup>a</sup>, Adrián M.T. Silva<sup>b</sup>, José L. Figueiredo<sup>b</sup>, Joaquim L. Faria<sup>b</sup>, Helder T. Gomes<sup>a,\*</sup>

<sup>a</sup> Laboratory of Separation and Reaction Engineering – Laboratory of Catalysis and Materials (LSRE-LCM), Escola Superior de Tecnologia e Gestão, Instituto Politécnico de Bragança, Campus de Santa Apolónia, 5300-253 Bragança, Portugal

<sup>b</sup> Laboratory of Separation and Reaction Engineering – Laboratory of Catalysis and Materials (LSRE-LCM), Departamento de Engenharia Química, Faculdade de Engenharia, Universidade do Porto, Rua Dr. Roberto Frias s/n, 4200-465 Porto, Portugal

## ARTICLE INFO

## Article history:

Received 6 April 2017

Received in revised form 14 July 2017

Accepted 23 July 2017

Available online 25 July 2017

## Keywords:

Lignin  
Physical activation  
Activated carbon  
CWPO  
 $H_2O_2$  efficiency

## ABSTRACT

A wheat and hemp lignin, obtained from a soda pulping-precipitation process, was carbonized at 800 °C under N<sub>2</sub> atmosphere. The resulting carbon material was thermally activated under oxidative atmosphere at four different temperatures (150, 200, 300 and 350 °C). The materials prepared at higher activation temperatures (300 and 350 °C) have proven their potential in the elimination of 4-nitrophenol (4-NP) from aqueous model solutions (5 g L<sup>-1</sup>) when using catalytic wet peroxide oxidation (CWPO). In these conditions we were able to remove around 70% of 4-NP after 24 h, with an efficient H<sub>2</sub>O<sub>2</sub> decomposition, in experiments conducted at relatively mild operating conditions (atmospheric pressure, 50 °C, pH = 3, catalyst load = 2.5 g L<sup>-1</sup> and [H<sub>2</sub>O<sub>2</sub>]<sub>0</sub> = 17.8 g L<sup>-1</sup>). By increasing the working temperature to 80 °C, complete 4-NP removal was obtained within 48 h (against 93% 4-NP removal at 50 °C), with an efficiency of H<sub>2</sub>O<sub>2</sub> consumption of 70% and a significant mineralization (61%). On the other hand, the materials prepared at lower activation temperatures (150 and 200 °C), with higher basicity, promote the faster but inefficient H<sub>2</sub>O<sub>2</sub> decomposition, 4-NP removal being lower than 25% after 24 h at 50 °C in CWPO. This can be attributed to the formation of species other than HO<sup>•</sup> radicals during H<sub>2</sub>O<sub>2</sub> decomposition, the recombination of the formed radicals into non-reactive species and a poor adsorption capacity.

© 2017 Elsevier B.V. All rights reserved.

## 1. Introduction

Lignin is one of the most abundant organic polymers in nature, and is obtained in large amounts as a residue of the pulp and paper industry and from the emerging lignocellulosic biorefineries (5–36 × 10<sup>8</sup> T/year) [1,2]. Due to its high-energy content, a major part of this industrial lignin, the so-called technical lignin, is combusted for heat recovery or used as an alternative fuel [3]. Nevertheless, the utilization of lignin as a fuel is not economically rational [4], and the development of alternative uses for lignin has been expanding in recent years, being increasingly applied as a starting material for the production of chemical compounds [3]. Due to its high carbon content and to a structure similar to that of bituminous coal [2,5], lignin seems to be an adequate precursor for the production of activated carbon materials. Several examples devoted to the preparation of activated carbons from lignin, using

different procedures, including physical and chemical activation [5–8] can be found in the literature. Highly porous materials have been developed, with specific surface areas as high as 2000 m<sup>2</sup> g<sup>-1</sup> and adsorbent capacities comparable to those reported for a number of commercial activated carbons [9]. The use of organic wastes as raw materials pursues the objective of building sustainable science.

Advanced oxidation processes (AOPs), primarily based on the action of hydroxyl radicals (HO<sup>•</sup>) to oxidize organic pollutants, are regarded as promising solutions for the treatment of aqueous effluents containing recalcitrant and non-biodegradable compounds [10,11]. These compounds are found in many industrial wastewater, such as those generated in pharmaceutical, petrochemical, dyes and paper industries, and are particularly difficult to remove by conventional biological processes when present at high concentrations (1–10 g L<sup>-1</sup>) [12]. Among the AOPs, catalytic wet peroxide oxidation (CWPO) uses hydrogen peroxide (H<sub>2</sub>O<sub>2</sub>) and a suitable catalyst to promote the formation of HO<sup>•</sup> for the degradation of the organic species under relatively mild operation conditions (0.1–0.2 MPa, 20–130 °C).

\* Corresponding author.

E-mail address: [htgomes@ipb.pt](mailto:htgomes@ipb.pt) (H.T. Gomes).

The classical heterogeneous catalysts employed in CWPO consist of a metallic active phase, mainly Fe-based, supported on a porous material (e.g. activated carbons, pillared clays and zeolites). However, these catalysts usually suffer from severe deactivation due to the leaching of the metallic phase to the reaction medium, with further steps being needed in the overall treatment process in order to remove or recover the metals from the treated wastewaters. This has led, in recent years, to the development of metal-free materials capable of catalyzing the decomposition of  $\text{H}_2\text{O}_2$  into radical species. In this context, carbonaceous materials have been found to be suitable metal-free catalysts for the CWPO process, promising results being obtained, both in terms of activity and stability [13–16].

In this study, organic agro-industrial wastes are used as raw materials for the development of carbonaceous materials and, to the best of our knowledge, the use of activated carbons produced from lignin as metal-free catalysts is assessed for the first time for the CWPO of wastewaters with high pollutant concentration. A 4-nitrophenol (4-NP) model solution (with a concentration of  $5\text{ g L}^{-1}$ ) was used to mimic a high-strength wastewater.

## 2. Experimental

### 2.1. Chemicals

The technical lignin used in this work, *Sarkanda* lignin, is a non-wood (wheat and hemp) lignin resulting from a soda pulping-precipitation process, patented by *Granit S.A.* This lignin was thoroughly characterized in previous works [17,18]. It is a *p*-hydroxyphenyl-guaiacyl-syringyl (HGS) lignin, characterized by high sugar and acid contents, 5.0% and  $0.62\text{ mmol g}^{-1}$ , respectively. Moreover, it presents an ash content of 3.3% (w/w) and phenolic and total hydroxyl contents of  $2.41\text{ mmol g}^{-1}$  and  $5.26\text{ mmol g}^{-1}$ , respectively. Other interesting features are the high nitrogen content (1.14%) and high thermal stability. *Sarkanda* lignin, purchased from *Granit S.A.*, was used as received, without further purification. The main reactants involved in the CWPO process under study, 4-NP (98 wt.%) and  $\text{H}_2\text{O}_2$  (30%, w/v), were purchased from *Acros Organics* and *Fluka*, respectively. Working standard solutions of formic acid (98 wt.%; *Panreac*), acetic acid (glacial acetic acid, 99.8 wt.%; *Fisher Chemical*), oxalic acid, malonic acid, maleic acid, malic acid, hydroquinone, phenol (all 99 wt.%; *Sigma-Aldrich*), 1,4-benzoquinone (99.5 wt.%; *Fluka*), catechol (98 wt.%; *Fluka*) and 4-nitrocatechol (98 wt.%; *Fluka*) were prepared and used for calibration in high-performance liquid chromatography (HPLC). Methanol (HPLC grade, 99.99 wt.%; *Fisher Chemical*), glacial acetic acid (HPLC grade, 99.99 wt.%; *Fisher Chemical*), acetonitrile (HPLC grade, 99.99 wt.%; *Fisher Chemical*) and sulphuric acid ( $\text{H}_2\text{SO}_4$ , 96–98 wt.%; *Riedel-de-Haen*) were used to prepare the mobile phases required for HPLC. Other reactants used were sodium hydroxide ( $\text{NaOH}$ , 98 wt.%; *Panreac*), sodium chloride ( $\text{NaCl}$ , 99 wt.%; *Sigma-Aldrich*), hydrochloric acid ( $\text{HCl}$ , 37 wt.%; *Sigma-Aldrich*), titanium (IV) oxysulphate (99.99%; *Sigma-Aldrich*), sodium sulphite ( $\text{Na}_2\text{SO}_3$ , 98 wt.%; *Sigma-Aldrich*) and phenolphthalein. All chemicals were used as received without further purification. Distilled water was used throughout the work except for mobile phase preparation, where ultrapure water was employed.

### 2.2. Synthesis of carbon materials

The initial carbon material was prepared by carbonizing the *Sarkanda* lignin under  $\text{N}_2$  atmosphere ( $100\text{ cm}^3\text{ min}^{-1}$ ) at  $120\text{ }^\circ\text{C}$  for 60 min, followed by  $400\text{ }^\circ\text{C}$  (60 min),  $600\text{ }^\circ\text{C}$  (60 min) and  $800\text{ }^\circ\text{C}$  (240 min), defining heating ramps of  $2\text{ }^\circ\text{C min}^{-1}$  between temperatures. The resulting carbon, ground to 0.10–0.25 mm, was named

LG. The carbon material LG was subsequently thermally activated under air atmosphere ( $100\text{ cm}^3\text{ min}^{-1}$ ) for 60 min at activation temperatures in the range  $150$ – $350\text{ }^\circ\text{C}$ , to obtain materials with different textural properties and surface chemistry. The as prepared activated carbons were named LG followed by a number corresponding to the activation temperature used (i.e. LG150, LG200, LG300 and LG350). The burn-off due to the thermal activation ranges from 16 wt.% (LG150) to 50 wt.% (LG350).

### 2.3. Characterization

Elemental analyses were performed on an *Elementar Vario MICRO Cube* system. The samples were previously dried at  $120\text{ }^\circ\text{C}$  in an oven to remove any water.

$\text{N}_2$  adsorption–desorption isotherms ( $-196\text{ }^\circ\text{C}$ ) were obtained to characterize the textural properties of the materials (*Quantachrome Nova4200e*). The samples were previously outgassed for 6 h at  $150\text{ }^\circ\text{C}$ . The specific surface area ( $S_{\text{BET}}$ ) was calculated by the BET equation, and the micropore volume ( $V_{\text{micro}}$ ) was obtained using the t-method [19].

The pH of point of zero charge ( $\text{pH}_{\text{PZC}}$ ) was determined by pH drift tests adapting the procedure described elsewhere [20]. Briefly, five  $\text{NaCl}$  (0.01 M) solutions were prepared as electrolyte with varying initial pH (in the range 2–11, using  $\text{HCl}$  and  $\text{NaOH}$  0.1 M solutions). 0.05 g of carbon sample was contacted with 20 mL of each  $\text{NaCl}$  solution. The equilibrium pH of each suspension was measured after 48 h under stirring (320 rpm) at room temperature. The  $\text{pH}_{\text{PZC}}$  value was determined by intercepting the curve 'final pH vs initial pH' with the straight line 'initial pH = final pH'.

The contents of acidic and basic sites were determined by titration as described elsewhere [20]. To measure the acidic sites, 0.2 g of the carbon sample were added to 25 mL of a  $\text{NaOH}$  (0.02 M) solution and left under stirring for 48 h (320 rpm) at room temperature. After filtering to remove the solid material, 20 mL of the remaining solution (with the residual  $\text{HO}^-$ ) were titrated with a  $\text{HCl}$  (0.02 M) solution. Similarly, to measure the basic sites 0.2 g of the carbon sample were added to 25 mL of  $\text{HCl}$  (0.02 M), this time the titration being done with a  $\text{NaOH}$  (0.02 M) solution. The amounts of acidic ( $C_a$ ) and basic ( $C_b$ ) sites were determined using the following expressions:

$$C_a = \frac{(\text{initial moles of NaOH}) - (\text{final moles of NaOH})}{\text{grams of material}} \quad (1)$$

$$C_b = \frac{(\text{initial moles of HCl}) - (\text{final moles of HCl})}{\text{grams of material}} \quad (2)$$

Temperature programmed desorption (TPD) analyses were performed by heating 0.1 g of the carbon sample, placed in a quartz tube, at  $5\text{ }^\circ\text{C min}^{-1}$  from room temperature up to  $1100\text{ }^\circ\text{C}$  under  $\text{N}_2$  atmosphere ( $1000\text{ cm}^3\text{ min}^{-1}$ ). The oxygenated surface groups present in each sample decompose as  $\text{CO}$  and/or  $\text{CO}_2$  [21], their concentrations being monitored during the thermal analysis using a *SIEMENS Ultramat 22* gas analyzer. Peaks deconvolution of the TPD profiles were adjusted to multiple Gaussian functions by *Origin Pro 9.0* software.

### 2.4. 4-Nitrophenol removal experiments

The CWPO runs were conducted in a batch reaction system described elsewhere [22], consisting of a 250 mL magnetically stirred (600 rpm) glass reactor, immersed in an oil bath with temperature control, and equipped with a reflux condenser and a sample collection port. In a typical experiment, the reactor was loaded with 50 mL of a 4-NP aqueous solution ( $5\text{ g L}^{-1}$ ) and heated to  $50\text{ }^\circ\text{C}$ . After temperature stabilization, the pH was adjusted to 3 using  $\text{H}_2\text{SO}_4$  and  $\text{NaOH}$  solutions, and the stoichiometric concen-

tration of  $\text{H}_2\text{O}_2$  ( $17.8 \text{ g L}^{-1}$ ), needed to completely mineralize the 4-NP, was incorporated to the system. The reaction started with the addition of  $0.125 \text{ g}$  of catalyst, corresponding to a catalyst load of  $2.5 \text{ g L}^{-1}$ . After  $24 \text{ h}$  of reaction, the catalyst was separated by filtration ( $20 \mu\text{m}$ , *Prat Dumas*), washed with distilled water and dried at  $60^\circ\text{C}$ . A blank experiment, *i.e.* without catalyst, was carried out to assess possible non-catalytic oxidation reactions promoted by  $\text{H}_2\text{O}_2$ . On the other hand, the capacity of the different synthesized carbon materials to adsorb 4-NP was evaluated by means of pure adsorption experiments, in which the operating conditions used in the CWPO runs were reproduced, but replacing  $\text{H}_2\text{O}_2$  by an equivalent volume of distilled water. The experiments were performed in triplicate, the standard deviation being less than 5% in all cases.

The performance of the catalysts was evaluated in terms of 4-NP,  $\text{H}_2\text{O}_2$  and total organic carbon (TOC) conversions, concentration of byproducts, and efficiency of  $\text{H}_2\text{O}_2$  consumption to mineralize the pollutant ( $\eta_{\text{H}_2\text{O}_2}$ ), defined as the TOC removal ( $X_{\text{TOC}}$  in%) per unit of  $\text{H}_2\text{O}_2$  decomposed ( $X_{\text{H}_2\text{O}_2}$  in%) [13]:

$$\eta_{\text{H}_2\text{O}_2} = \frac{X_{\text{TOC}}}{X_{\text{H}_2\text{O}_2}} \cdot 100 \quad (3)$$

## 2.5. Analytical methods

Small aliquots of the resulting effluent were withdrawn from the reactor at different reaction times for analysis (typically at 0, 5, 15, 30, 60, 120, 240, 480 min, and 24 h).

The concentrations of 4-NP and the intermediates and/or byproducts derived from its oxidation were identified and quantified by HPLC, using a *Jasco* system equipped with an UV/VIS detector (*UV-2075 Plus*) and a quaternary gradient pump (*PU-2089 Plus*) for solvent delivery. An excess of  $\text{Na}_2\text{SO}_3$  was immediately added to the effluent samples to consume the residual  $\text{H}_2\text{O}_2$ , and the catalyst was removed by filtration to stop the reaction. For the determination of 4-NP and the aromatic intermediates, a *Kromasil 100-5-C18 column* ( $15 \text{ cm} \times 4.6 \text{ mm}$ ;  $5 \mu\text{m}$  particle size), working at room temperature, was used as stationary phase, and the mobile phase used was an A:B (40:60) mixture of 3% acetic acid and 1% acetonitrile in methanol (A) and 3% acetic acid in ultrapure water (B), at a flowrate of  $1 \text{ mL min}^{-1}$ . For the determination of the carboxylic acids, a *YMC-Triart C18 column* ( $25 \text{ cm} \times 4.6 \text{ mm}$ ;  $5 \mu\text{m}$  particle size) was used with a mobile phase consisting of an A:B (95:5) mixture of 1%  $\text{H}_2\text{SO}_4$  in ultrapure water (A) and acetonitrile (B) operating in isocratic mode at  $0.6 \text{ mL min}^{-1}$ . The absorbance wavelength was adjusted to 318 nm for the determination of 4-NP, 277 nm for the aromatic intermediates and 210 nm for the carboxylic acids.

Additionally, a colorimetric method was used to follow the concentration of  $\text{H}_2\text{O}_2$  along the reaction course by means of UV/VIS spectrophotometry (*T70 spectrometer*, *PG Instruments Ltd.*). The effluent samples were filtered to remove the catalyst and acidified with a  $\text{H}_2\text{SO}_4$  0.5 M solution. Then,  $0.1 \text{ mL}$  of titanium oxysulfate was added, and the absorbance was measured at 405 nm [23].

Finally, the TOC content was determined using a *Shimadzu TOC-L* analyzer.

## 3. Results and discussion

### 3.1. Characterization

The elemental composition (% w/w) of the *Sarkanda* lignin is given in **Table 1**, where a significant presence of oxygen in its composition is notorious, which is in line with the amount of hydroxyl groups that characterize the molecular structure of this type of raw materials. The presence of oxygen substantially diminishes in the carbonized LG, due to the release of volatile matter during the thermal treatment, increasing the carbon proportion. Nevertheless,

**Table 1**

Composition (% w/w) of *Sarkanda* lignin and carbonaceous materials LG, LG150, LG200, LG300 and LG350, as determined by elemental analysis.

	C	H	N	S	O*
Lignin	58.79	5.76	1.05	0.85	33.55
LG	77.65	1.73	1.46	1.03	18.13
LG150	79.12	1.74	1.49	1.10	16.55
LG200	76.96	1.74	1.45	1.08	18.76
LG300	71.98	1.92	1.55	1.49	23.06
LG350	68.76	2.09	1.59	1.71	25.85

\* difference to 100%

**Table 2**

Textural properties of the prepared activated carbons.

Catalyst	$S_{\text{BET}}$ ( $\text{m}^2 \text{ g}^{-1}$ )	$V_{\text{micro}}$ ( $\text{cm}^3 \text{ g}^{-1}$ )	$S_{\text{meso}}$ ( $\text{m}^2 \text{ g}^{-1}$ )
LG	5	0	5
LG150	12	0	12
LG200	260	0.12	18
LG300	395	0.21	29
LG350	539	0.26	74

**Table 3**

Surface chemical properties of the prepared activated carbons.

Catalyst	$\text{pH}_{\text{PZC}}$	basicity ( $\mu\text{mol g}^{-1}$ )	acidity ( $\mu\text{mol g}^{-1}$ )	b:a
LG	8.7	1193	246	4.9
LG150	8.9	1383	343	4.0
LG200	9.8	1288	418	3.1
LG300	8.7	1020	534	1.9
LG350	8.3	823	697	1.2

oxygen content progressively increases again after the treatment under air atmosphere at increasing temperatures, probably due to the incorporation of oxygenated groups in the activated carbons surfaces.

Regarding the textural properties (**Table 2**), the  $\text{N}_2$  adsorption-desorption analysis of LG reveals a non-porous material, with a  $S_{\text{BET}}$  of  $5 \text{ m}^2 \text{ g}^{-1}$ . Thermal activation, particularly above  $200^\circ\text{C}$ , generates a significant porosity, essentially microporous in character, progressively developed as the activation temperature increases, until *ca.*  $540 \text{ m}^2 \text{ g}^{-1}$  for LG350. When compared to the  $5 \text{ m}^2 \text{ g}^{-1}$  of LG, LG350 reveals a higher than 100-fold porosity development, which may assist its sorption capacity. The properties of the obtained carbons are highly influenced by the activating agent, time and temperature employed [24–29]. Ribeiro et al. reported similar  $S_{\text{BET}}$  (up to  $598 \text{ m}^2 \text{ g}^{-1}$ ) in activated carbons prepared from glycerol using the same procedure [25].

Regarding the surface chemistry, **Table 3** summarizes the  $\text{pH}_{\text{PZC}}$  and the amount of acidic and basic sites present in the surface of the prepared carbon materials. The basic character of the initial LG is noteworthy, with *ca.*  $1200 \mu\text{mol g}^{-1}$  of basic surface groups and a  $\text{pH}_{\text{PZC}}$  of 8.7, corresponding to a basicity/acidity ratio of 4.85. The contents of acidic functionalities increase with the activation temperature, suggesting the incorporation of more acidic oxygenated groups during the treatment under air atmosphere. Nevertheless, in spite of this gradual increase of acidity, all the activated carbons show a large content of basic groups. This remarkable basic character is corroborated by the  $\text{pH}_{\text{PZC}}$  values obtained, between 8.3 and 9.8 for all the materials, and with a ratio basicity/acidity (b:a, **Table 3**) between 1.2 and 4.9. Basic carbon materials are known to be more active in the decomposition of  $\text{H}_2\text{O}_2$  [30,31]. Therefore, all the prepared activated carbons are expected to be appropriate for the CWPO process.

To characterize the surface chemistry, the different functional groups present at the carbon surface were identified and quantified by deconvolution of the TPD profiles shown in **Fig. 1**, according to the procedure described elsewhere [21]. The peaks

**Table 4**

Total amounts of  $\text{CO}_2$  and CO obtained during TPD analysis and amounts of the different functional groups from deconvolution of TPD profiles.

Catalyst	$\text{CO}_2$ ( $\mu\text{mol g}^{-1}$ )	CO ( $\mu\text{mol g}^{-1}$ )	carboxylic ( $\mu\text{mol g}^{-1}$ )	lactone ( $\mu\text{mol g}^{-1}$ )	anhydride ( $\mu\text{mol g}^{-1}$ )	phenol ( $\mu\text{mol g}^{-1}$ )	ether ( $\mu\text{mol g}^{-1}$ )	carbonyl/quinone ( $\mu\text{mol g}^{-1}$ )
LG	784	1935	354	174	153	118	243	870
LG150	875	2018	254	73	465	148	360	597
LG200	769	2325	230	47	488	128	367	839
LG300	624	4338	180	170	583	538	787	1142
LG350	976	4542	197	309	916	711	813	1812

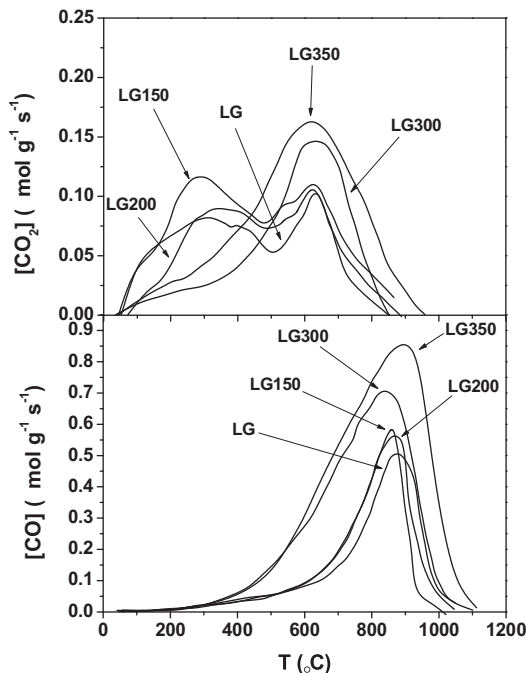


Fig. 1. TPD profiles of the carbon materials:  $\text{CO}_2$  (top) and CO (bottom).

appearing in the  $\text{CO}_2$ -TPD profiles can be assigned to carboxylic acids (peak in the range 270–350  $^{\circ}\text{C}$ ), carboxylic anhydrides (440–590  $^{\circ}\text{C}$ ) and lactones (620–710  $^{\circ}\text{C}$ ), whilst the peaks in the CO-TPD profiles are related to carboxylic anhydrides (440–590  $^{\circ}\text{C}$ ), phenols (620–680  $^{\circ}\text{C}$ ), ethers (740–770  $^{\circ}\text{C}$ ) and carbonyls/quinones (850–900  $^{\circ}\text{C}$ ). The amounts of the different functional groups in each carbon material are shown in Table 4. The larger area of the peak associated with carbonyl and/or quinone groups in all the samples should be noted. The presence of large amounts of quinones may explain the strong basic character of the materials developed. The results show a clear increase of oxygenated groups with the increase of the thermal activation temperature, mainly manifested in the form of carboxylic anhydrides and phenols, which contribute to the progressive enhancement in the acidity observed before (Table 3).

### 3.2. Catalytic performance in CWPO experiments

The prepared activated carbons were used as metal-free catalysts in the CWPO of highly-concentrated 4-NP solutions.

The profiles of removal of 4-NP and decomposition of  $\text{H}_2\text{O}_2$  as function of the catalyst are shown in Fig. 2. As can be seen, the behavior of the catalysts prepared at higher and lower activation temperatures is quite different. The catalysts prepared at higher activation temperatures (300 and 350  $^{\circ}\text{C}$ ) are more efficient in removing 4-NP ( $X \approx 70\%$ ), in spite of a modest  $\text{H}_2\text{O}_2$  decomposition rate. On the other hand, the materials prepared at low activation temperatures (150 and 200  $^{\circ}\text{C}$ ), and the non-activated

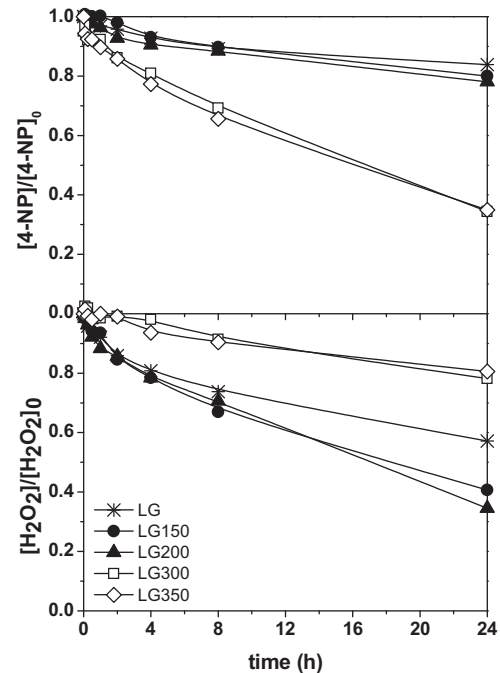


Fig. 2. Normalized concentration evolution of 4-NP (top) and  $\text{H}_2\text{O}_2$  (bottom) during the CWPO experiments (normalized for the corresponding initial concentrations). Operating conditions:  $C_{4\text{-NP}} = 5 \text{ g L}^{-1}$ ,  $C_{\text{H}_2\text{O}_2} = 17.8 \text{ g L}^{-1}$ ,  $C_{\text{cat}} = 2.5 \text{ g L}^{-1}$ ,  $\text{pH} = 3$ ,  $T = 50^{\circ}\text{C}$ .

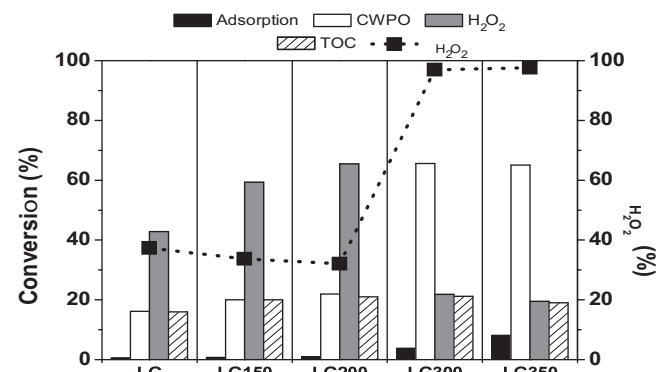
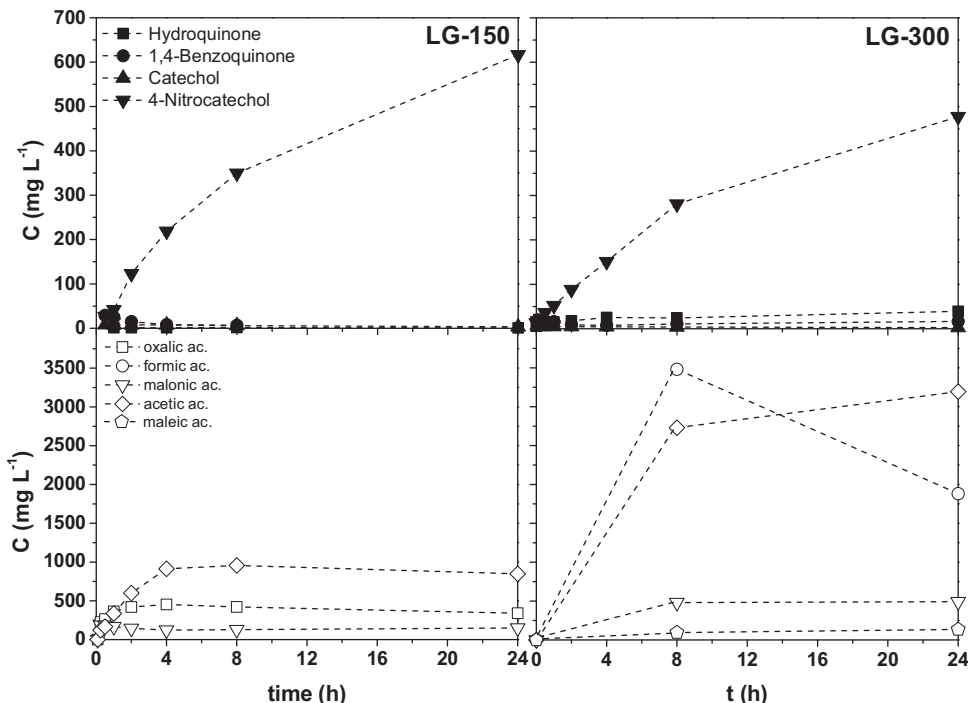


Fig. 3. Removal of 4-NP from aqueous solution by adsorption and by CWPO; TOC removal,  $\text{H}_2\text{O}_2$  decomposition and  $\eta_{\text{H}_2\text{O}_2}$  obtained in the CWPO experiments; results after 24 h. Operating conditions:  $C_{4\text{-NP}} = 5 \text{ g L}^{-1}$ ,  $C_{\text{H}_2\text{O}_2} = 17.8 \text{ g L}^{-1}$ ,  $C_{\text{cat}} = 2.5 \text{ g L}^{-1}$ ,  $\text{pH} = 3$ ,  $T = 50^{\circ}\text{C}$ .

carbon LG, remove less 4-NP ( $X_{4\text{-NP}} < 25\%$ ) in spite of the faster  $\text{H}_2\text{O}_2$  conversion.

The higher porosity development of LG300 and LG350 could explain the better 4-NP removal results, since a higher  $S_{\text{BET}}$  should favor the adsorption capacity. In order to discriminate this hypothesis, pure adsorption runs were done using the same operation conditions used in the CWPO tests, but without  $\text{H}_2\text{O}_2$ . Fig. 3 compares the results of 4-NP removal obtained after 24 h in the CWPO



**Fig. 4.** Concentration evolution of the reaction byproducts resulting from the CWPO of 4-NP with LG-150 (left) and LG-300 (right). Operating conditions:  $C_{4-NP} = 5 \text{ g L}^{-1}$ ,  $C_{H_2O_2} = 17.8 \text{ g L}^{-1}$ ,  $C_{\text{cat}} = 2.5 \text{ g L}^{-1}$ ,  $\text{pH} = 3$ ,  $T = 50^\circ\text{C}$ .

and adsorption runs. The  $\text{H}_2\text{O}_2$  and TOC conversions are also shown, as well as the  $\eta_{\text{H}_2\text{O}_2}$  efficiency.

As expected, the adsorption capacity of the activated carbons increases with the activation temperature, in the same order as the  $S_{\text{BET}}$  does. Nevertheless, the adsorption contribution to the removal of 4-NP ( $5 \text{ g L}^{-1}$ ) is negligible for all the tested activated carbons when compared to the removals observed in the CWPO experiments. The materials LG300 and LG350 show the highest adsorption capacity, with 4-NP removals of only 5% and 8%, respectively. It is thus concluded that the better results obtained with these two catalysts in the CWPO of 4-NP cannot be exclusively attributed to a better adsorption capacity, but also to their surface chemistry, presumably to its basic character.

Several authors reported that basic carbon materials lead to high  $\text{H}_2\text{O}_2$  decomposition rates in CWPO processes [14,30–32]. In addition, a previous study shows that the presence of basic groups in the carbon materials increases not only the  $\text{H}_2\text{O}_2$  decomposition rate, but also the yield of  $\text{HO}^\bullet$  formation [31]. Taking this into consideration, the higher 4-NP removals obtained in the present work with LG300 and LG350 suggest that the decomposition of  $\text{H}_2\text{O}_2$  is highly efficient for the generation of  $\text{HO}^\bullet$  radicals, responsible for the mineralization of 4-NP. This is confirmed by the values of  $\eta_{\text{H}_2\text{O}_2}$ , close to 100% with both catalysts. As stated before, the amounts of quinones determined by TPD in the materials prepared at higher activation temperatures are substantially higher than those related to low-temperature activated ones (Table 4). Also, there is a significantly higher amount of ether groups in the materials prepared at higher temperatures. Both types of surface groups may act as electron-donating functionalities, favoring the generation and efficient consumption of  $\text{HO}^\bullet$  radicals, resulting in the observed high values of  $\eta_{\text{H}_2\text{O}_2}$  for LG300 and LG350. In spite of the higher content of these specific basic functionalities in these materials, the amount of acidic groups is also higher, resulting in the lower global basicity observed for LG300 and LG350 when compared to the carbon materials activated at lower temperatures (LG150 and LG200), as shown in Table 3. On the other hand, LG150 and LG200, promoted

the faster decomposition of  $\text{H}_2\text{O}_2$ , in agreement with their higher basicity. However, the lower amount of quinones and ether groups in these cases, as well as the larger content of strong carboxylic acid groups, probably favors its decomposition into species other than  $\text{HO}^\bullet$  radicals [30–34], directly affecting the process efficiency,  $\eta_{\text{H}_2\text{O}_2}$  dropping to *ca.* 50%. This is in agreement with previous reports where a fast decomposition of  $\text{H}_2\text{O}_2$  is set to favor the formation of non-reactive species due to the recombination of the formed radicals into  $\text{H}_2\text{O}$  and  $\text{O}_2$  [22,35]. This, coupled to the low adsorption capacity of the materials, leads to a low 4-NP conversion, in spite of the better decomposition of  $\text{H}_2\text{O}_2$  observed. On the contrary, as explained above, the catalysts prepared at the higher activation temperatures, LG300 and LG350, which have a moderate basic character, promote the slow but efficient decomposition of  $\text{H}_2\text{O}_2$  into  $\text{HO}^\bullet$  radicals, which further attack the pollutant molecules. These materials decompose  $\text{H}_2\text{O}_2$  with a moderate rate, reaching a total decomposition of *ca.* 20% after 24 h. Consequently, the concentration of  $\text{HO}^\bullet$  radicals obtained is not high, limiting the oxidation of 4-NP. Despite obtaining a low concentration of  $\text{HO}^\bullet$ , the radicals formed are effectively used in the mineralization of 4-NP, since at the time these radicals are being formed, they attack the pollutants molecules. Since the concentration of  $\text{HO}^\bullet$  is not higher, the final result is not better. As will be seen in section 3.3, increasing the reaction time enhances the pollutant conversion, since higher amounts of 4-NP will be attacked.

Despite the effective formation of  $\text{HO}^\bullet$  radicals and the considerable 4-NP removal achieved with LG300 and LG350, the mineralization obtained is not remarkable with all the materials prepared. For the sake of comparison, Fig. 4 shows the concentration of the different reaction byproducts (aromatics and carboxylic acids) resulting from the CWPO with LG150 and LG300, respectively. The similar concentration in the aromatic intermediates formed, independently of the activation temperature, can be appreciated. The only notable difference between both catalysts lies in the carboxylic acids formed, since significantly higher concentrations of formic and acetic acids are observed with the catalyst

**Table 5**

Results obtained in the CWPO experiments with LG300 at different temperatures and times.

T (°C)	Time (h)	x <sub>4-NP</sub> (%)	x <sub>H<sub>2</sub>O<sub>2</sub></sub> (%)	x <sub>TOC</sub> (%)	η <sub>H<sub>2</sub>O<sub>2</sub></sub> (%)	Σ aromatics <sup>a</sup> (mg L <sup>-1</sup> )	Σ acids <sup>b</sup> (mg L <sup>-1</sup> )	C mismatch (%)
50	24	66	22	21	97	1104	1252	44
50	36	74	34	16	47	1151	1675	33
50	48	93	40	14	35	1249	2185	18
80	48	100	87	61	70	28	4166	6

<sup>a</sup> Sum of hydroquinone, 1,4-benzoquinone, catechol and 4-nitrocatechol.<sup>b</sup> Sum of oxalic acid, formic acid, malic acid, maleic acid and acetic acid.

prepared at higher activation temperatures (the same trend is observed with LG350, not shown), whereas a remarkable oxalic acid concentration was determined for the low-temperature prepared catalysts (the same is observed with LG200, not shown). This may be due to the higher extent of 4-NP conversion obtained with LG300 and LG350 when compared to LG150 and LG200, which consequently results in the formation of larger amounts of carboxylic acids. This coupled to the highly refractory nature of these compounds leads to higher accumulation of carboxylic acids in the CWPO experiments performed with LG300 and LG350. As an exception, oxalic acid, also known to be refractory to oxidation by CWPO [36], is not generated with LG300 and LG350, which represents an advantage for the process performance with these catalysts.

With regard to catalysts stability, preliminary studies with LG350 suggest that the catalyst suffers a gradual loss of activity upon reutilization, converting 65%, 58% and 44% of 4-NP after three consecutive uses. A possible explanation might be the highly oxidizing reaction environment, but additional studies are needed to confirm this hypothesis. Different authors have explored the deactivation causes of carbonaceous materials used as catalysts in CWPO, finding that catalytic active sites may be partially blocked during CWPO due to deposition of condensation by-products [37,38] or polymer-like material formed as a result of oxidative coupling of the organic pollutant and phenolic intermediates on the active carbon surface [33], provoking the progressive deactivation of the catalyst. Zazo et al. [33] also related the existence of these deposits to the formation of higher amounts of organic acids when increasing the temperature, since the temperature increase might lead to the oxidation of such polymer-like material to a higher extent, yielding organic acids. As will be seen in the next section, this is consistent with our own study.

### 3.3. Process intensification

The decomposition of H<sub>2</sub>O<sub>2</sub> is highly efficient for the generation and consumption of HO<sup>•</sup> radicals when catalyzed by LG300 and LG350, but their use did not promote a complete removal of 4-NP by CWPO within 24 h. In order to achieve complete 4-NP removal, a set of experiments were done with LG300 under intensified conditions, where the reaction temperature and time were increased to 80 °C and 48 h, respectively. Table 5 summarizes the results of 4-NP conversion (x<sub>4-NP</sub>), H<sub>2</sub>O<sub>2</sub> conversion (x<sub>H<sub>2</sub>O<sub>2</sub></sub>) and TOC conversion (x<sub>TOC</sub>), as well as the efficiency of H<sub>2</sub>O<sub>2</sub> consumption, η<sub>H<sub>2</sub>O<sub>2</sub></sub>, the aromatic byproducts (hydroquinone, 1,4-benzoquinone, catechol and 4-nitrocatechol) and the organic acids (formic, malic, maleic, acetic and oxalic acids) obtained at different reaction times. As observed, the increase of the reaction time favors the pollutant conversion, which is almost complete after 48 h of reaction at 80 °C. As expected, H<sub>2</sub>O<sub>2</sub> conversion also increases, but η<sub>H<sub>2</sub>O<sub>2</sub></sub> sharply diminishes, dropping from 97% to only 35%, due to the lower TOC conversion. On the other hand, the increase of the reaction temperature increases the kinetics of H<sub>2</sub>O<sub>2</sub> decomposition, resulting in a corresponding higher H<sub>2</sub>O<sub>2</sub> conversion and higher η<sub>H<sub>2</sub>O<sub>2</sub></sub> (increase from 35% at 50 °C to 70% at 80 °C, after 48 h). As a consequence, the conversions of 4-NP and TOC are improved,

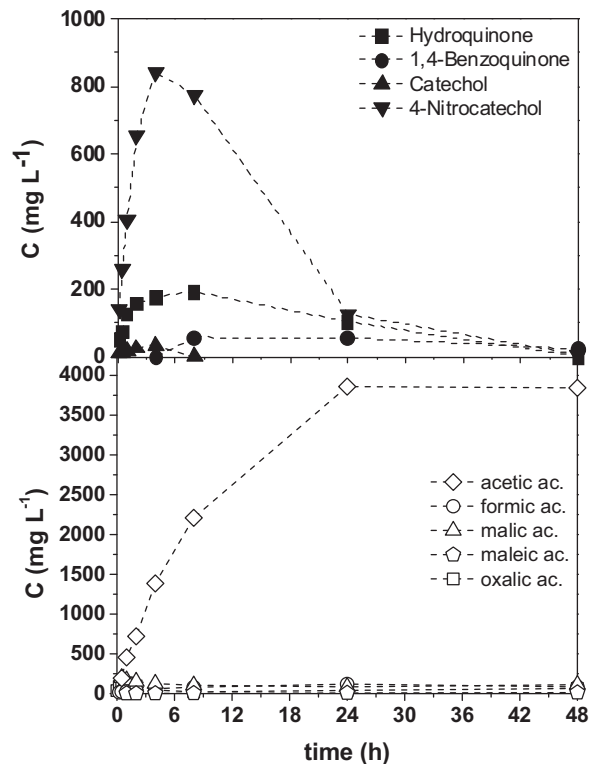


**Fig. 5.** Concentration evolution of the reaction byproducts resulting from the CWPO of 4-NP with LG-300 at 80 °C. Operating conditions: C<sub>4-NP</sub> = 5 g L<sup>-1</sup>, C<sub>H<sub>2</sub>O<sub>2</sub></sub> = 17.8 g L<sup>-1</sup>, C<sub>cat</sub> = 2.5 g L<sup>-1</sup>, pH = 3, T = 80 °C.

and the intermediates obtained are mainly low molecular weight carboxylic acids. The concentration evolution of the different intermediates formed during the CWPO at 80 °C is shown in Fig. 5, where the large amount of aromatics formed during the first 8 h can be noticed, especially 4-nitrocatechol, with a maximum concentration of 840 mg L<sup>-1</sup> after 6 h. Subsequently, the concentration of aromatic intermediates sharply diminishes, while the concentration of acetic acid steadily increases. As suggested before, deposition of condensation by-products or polymer-like material may be occurring, and part of this deposit may be desorbed again after the first 24 h under continuous operation. Because of the deposition of organic material, the carbon balance suffers a strong mismatch, which decreases from the 24-h-sample to the 48-h-sample, coherently with the desorption of organic deposits which contribute to TOC.

### 4. Conclusions

All the lignin-based carbon materials prepared in this work are active for the decomposition of H<sub>2</sub>O<sub>2</sub> and for the removal of 4-NP by CWPO.

The temperature used for the activation of the carbon materials plays an important role in the development of porosity and in the surface chemistry of the activated carbons generated. This

dependence is particularly evident in the materials activated at the higher temperatures, which present superior  $S_{\text{BET}}$  and lower basicity/ acidity ratios.

The activated carbons prepared at high activation temperatures (300 and 350 °C) promoted the efficient  $\text{H}_2\text{O}_2$  decomposition, removing around 70% of 4-NP in 24 h. On the other hand, the materials prepared at low activation temperatures (150 and 200 °C) promoted faster but inefficient  $\text{H}_2\text{O}_2$  decomposition, the 4-NP removal being lower than 25% after 24 h in these cases. This low efficiency is mainly attributed to the formation of species other than  $\text{HO}^\bullet$  radicals during  $\text{H}_2\text{O}_2$  decomposition, and to the recombination of the formed radicals into non-reactive species ( $\text{H}_2\text{O}$  and  $\text{O}_2$ ), as well as to the poor adsorption capacity of these materials.

Increasing the reaction temperature and time to 80 °C and 48 h, respectively, resulted in complete 4-NP removal, with high mineralization level and an efficiency of  $\text{H}_2\text{O}_2$  consumption,  $\eta_{\text{H}_2\text{O}_2}$ , of 70% with the catalyst activated at 300 °C.

## Acknowledgments

This work was financially supported by Project POCI-01-0145-FEDER-006984—Associate Laboratory LSRE-LCM, funded by FEDER through COMPETE2020 – Programa Operacional Competitividade e Internacionalização (POCI) – and by national funds through FCT – Fundação para a Ciência e a Tecnologia, and Project AIProcMat@N2020 – Advanced Industrial Processes and Materials for a Sustainable Northern Region of Portugal 2020, with the reference NORTE-01-0145-FEDER-000006, supported by Norte Portugal Regional Operational Programme (NORTE 2020), under the Portugal 2020 Partnership Agreement, through the European Regional Development Fund (FEDER). M. Martin Martinez and A.M.T. Silva acknowledge respectively financial support from the FCT Postdoctoral grant SFRH/BPD/108510/2015 and the FCT Investigator 2013 Programme F/01501/2013 with financing from the European Social Fund and the Human Potential Operational Programme.

## References

- G. Gellerstedt, G. Henriksson, Lignins Major sources, structure and properties, in: M.N. Belgacem, A. Gandini (Eds.), *Monomers, Polymers and Composites from Renewable Resources*, Elsevier, Amsterdam, 2008, pp. 201–224.
- M. Chávez-Sifontes, M.E. Domine, Lignin, structure and applications: depolymerization methods for obtaining aromatic derivatives of industrial interest, *Av. Cienc. Ing.* 4 (4) (2013) 15–46.
- X. Tian, Z. Fang, R.L. Smith, Z. Wu Jr., M. Liu, Properties, chemical characteristics and application of lignin and its derivatives, in: Z. Fang, R.L. Smith Jr. (Eds.), *Production of Biofuels and Chemicals from Lignin*, Springer Singapore, Singapore, 2016, pp. 3–33.
- A. Vishtal, A. Kraslawski, Challenges in industrial applications of technical lignins, *BioResources* 6 (3) (2011) 3547–3568.
- J.J. Rodriguez, T. Cordero, J. Rodríguez-Mirasol, Carbon materials from lignin and their applications, in: Z. Fang, R.L. Smith Jr. (Eds.), *Production of Biofuels and Chemicals from Lignin*, Springer Singapore, Singapore, 2016, pp. 217–262.
- L.M. Cotoruelo, M.D. Marqués, F.J. Díaz, J. Rodríguez-Mirasol, T. Cordero, J.J. Rodriguez, Activated carbons from lignin: their application in liquid phase adsorption, *Sep. Sci. Technol.* 42 (2007) 3363–3389.
- J.A. Zazo, J. Bedia, C.M. Fierro, G. Pliego, J.A. Casas, J.J. Rodriguez, Highly stable Fe on activated carbon catalysts for CWPO upon  $\text{FeCl}_3$  activation of lignin from black liquors, *Catal. Today* 187 (2012) 115–121.
- M.R. Snowdon, A.K. Mohanty, M. Misra, A Study of carbonized lignin as an alternative to carbon black, *ACS Sustain. Chem. Eng.* 2 (2014) 1257–1263.
- P.J.M. Suhas, M.M.L. Carrott, Ribeiro Carrott, Lignin – from natural adsorbent to activated carbon: a review, *Bioresour. Technol.* 98 (2007) 2301–2312.
- R. Andreozzi, V. Caprio, A. Insola, R. Marotta, Advanced oxidation processes (AOP) for water purification and recovery, *Catal. Today* 53 (1999) 51–59.
- G. Pliego, J.A. Zazo, P. García-Munoz, M. Muñoz, J.A. Casas, J.J. Rodriguez, Trends in the intensification of the Fenton process for wastewater treatment: an overview, *Crit. Rev. Environ. Sci. Technol.* 45 (2015) 2611–2692.
- S. Azabou, W. Najjar, M. Bouaziz, A. Ghorbel, S. Sayadi, A compact process for the treatment of olive mill wastewater by combining wet hydrogen peroxide catalytic oxidation and biological techniques, *J. Hazard. Mater.* 183 (2010) 62–69.
- R.S. Ribeiro, A.M.T. Silva, L. Pastrana-Martinez, J.L. Figueiredo, J.L. Faria, H.T. Gomes, Graphene-based materials for the catalytic wet peroxide oxidation of highly concentrated 4-nitrophenol solutions, *Catal. Today* 249 (2015) 204–212.
- F. Lücking, H. Köser, M. Jank, A. Ritter, Iron powder, graphite and activated carbon as catalysts for the oxidation of 4-chlorophenol with hydrogen peroxide in aqueous solution, *Water Res.* 32 (1998) 2607–2614.
- C.M. Domínguez, P. Ocón, A. Quintanilla, J.A. Casas, J.J. Rodriguez, Graphite and carbon black as catalysts for wet peroxide oxidation, *Appl. Catal. B* 144 (2014) 599–606.
- A. Dhaouadi, N. Adhoum, Heterogeneous catalytic wet peroxide oxidation of paraquat in the presence of modified activated carbon, *Appl. Catal. B* 97 (2010) 227–235.
- C.A. Cateto, M.F. Barreiro, A.E. Rodrigues, M.C. Brochier-Salon, W. Thielemans, M.N. Belgacem, Lignins as macromonomers for polyurethane synthesis: a comparative study on hydroxyl group determination, *J. Appl. Polym. Sci.* 109 (2008) 3008–3017.
- C.A. Cateto, M.F. Barreiro, A.E. Rodrigues, M.N. Belgacem, Optimization study of lignin oxypropylation in view of the preparation of polyurethane rigid foams, *Ind. Eng. Chem. Res.* 48 (2009) 2583–2589.
- S. Brunauer, P.H. Emmett, E. Teller, Adsorption of gases in multimolecular layers, *J. Am. Chem. Soc.* 60 (1938) 309–319.
- H.T. Gomes, S.M. Miranda, M.J. Sampaio, A.M.T. Silva, J.L. Faria, Activated carbons treated with sulphuric acid: catalysts for catalytic wet peroxide oxidation, *Catal. Today* 151 (2010) 153–158.
- J.L. Figueiredo, M.F.R. Pereira, M.M.A. Freitas, J.J.M. Órfão, Modification of the surface chemistry of activated carbons, *Carbon* 37 (1999) 1379–1389.
- M. Martin-Martinez, R.S. Ribeiro, B.F. Machado, P. Serp, S. Morales-Torres, A.M.T. Silva, J.L. Figueiredo, J.L. Faria, H.T. Gomes, Role of nitrogen doping on the performance of carbon nanotube catalysts: a catalytic wet peroxide oxidation application, *ChemCatChem* 8 (2016) 2068–2078.
- W.C. Ketchie, Y. Fang, M.S. Wong, M. Murayama, R.J. Davis, Influence of gold particle size on the aqueous-phase oxidation of carbon monoxide and glycerol, *J. Catal.* 250 (2007) 94–101.
- J. Rodriguez-Mirasol, T. Cordero, J.J. Rodriguez, Activated carbons from carbon dioxide partial gasification of eucalyptus kraft lignin, *Energy Fuels* 7 (1993) 133–138.
- R.S. Ribeiro, A.M.T. Silva, M.T. Pinho, J.L. Figueiredo, J.L. Faria, H.T. Gomes, Development of glycerol-based metal-free carbon materials for environmental catalytic applications, *Catal. Today* 240 (2015) 61–66.
- R. Helleur, N. Popovic, M. Ikura, M. Stanciulescu, D. Liu, Characterization and potential applications of pyrolytic char from ablative pyrolysis of used tires, *J. Anal. Appl. Pyrolysis* 58–59 (2001) 813–824.
- N.K. Hamadi, X.D. Chen, M.M. Farid, M.G.Q. Lu, Adsorption kinetics for the removal of chromium (VI) from aqueous solution by adsorbents derived from used tyres and sawdust, *Chem. Eng. J.* 84 (2001) 95–105.
- P. Ariyadejwanich, W. Tanthanapichakoon, K. Nakagawa, S.R. Mukai, H. Tamon, Preparation and characterization of mesoporous activated carbon from waste tires, *Carbon* 41 (2003) 157–164.
- G. San Miguel, G.D. Fowler, C.J. Sollars, A study of the characteristics of activated carbons produced by steam and carbon dioxide activation of waste tire rubber, *Carbon* 41 (2003) 1009–1016.
- V.P. Santos, M.F.R. Pereira, P.C.C. Faria, J.J.M. Órfão, Decolourisation of dye solutions by oxidation with  $\text{H}_2\text{O}_2$  in the presence of modified activated carbons, *J. Hazard. Mater.* 162 (2009) 736–742.
- R.S. Ribeiro, A.M.T. Silva, J.L. Figueiredo, J.L. Faria, H.T. Gomes, The influence of structure and surface chemistry of carbon materials on the decomposition of hydrogen peroxide, *Carbon* 62 (2013) 97–108.
- L.B. Khalil, B.S. Girgis, T.A. Tawfik, Decomposition of  $\text{H}_2\text{O}_2$  on activated carbon obtained from olive stones, *J. Chem. Technol. Biotechnol.* 76 (2001) 1132–1140.
- J.A. Zazo, J.A. Casas, A.F. Mohedano, J.J. Rodriguez, Catalytic wet peroxide oxidation of phenol with a Fe/active carbon catalyst, *Appl. Catal. B* 65 (2006) 261–268.
- G.V. Buxton, C.L. Greenstock, W.P. Helman, A.B. Ross, Critical Review of rate constants for reactions of hydrated electrons, hydrogen atoms and hydroxyl radicals  $\text{OH}/\text{O}^\bullet$  in Aqueous Solution, *J. Phys. Chem. Ref. Data* 17 (1988) 513–886.
- A.J. Elliot, G.V. Buxton, Temperature dependence of the reactions  $\text{OH} + \text{O}^\bullet$  and  $\text{OH} + \text{HO}_2$  in water up to 200 °C, *J. Chem. Soc. Faraday Trans.* 88 (1992) 2465–2470.
- A. Rey, M. Faraldo, J.A. Casas, J.A. Zazo, A. Bahamonde, J.J. Rodriguez, Catalytic wet peroxide oxidation of phenol over Fe/AC catalysts: influence of iron precursor and activated carbon surface, *Appl. Catal. B* 86 (2009) 69–77.
- C.M. Domínguez, P. Ocón, A. Quintanilla, J.A. Casas, J.J. Rodriguez, *Appl. Catal. B* 140 (2013) 663–670.
- Rui S. Ribeiro, Adrián M.T. Silva, Pedro B. Tavares, José L. Figueiredo, Joaquim L. Faria, Helder T. Gomes, Hybrid magnetic graphitic nanocomposites for catalytic wet peroxide oxidation applications, *Cat. Today* 280 (2017) 184–191.